

## Fabrication and characterization of zinc oxide nanoparticles for photocatalytic application

S. Haq<sup>a,\*</sup>, M. B. Ali<sup>b</sup>, A. Mezni<sup>c</sup>, A. Hedfi<sup>b</sup>, W. Rehman<sup>d</sup>, Gh. Sarwar<sup>d</sup>, Zain-ul-Abdin<sup>a</sup>, S. U. Din<sup>a</sup>, F. U. Rehman<sup>a</sup>, S. A. Abbasi<sup>a</sup>, A. L. Lone<sup>a</sup>

<sup>a</sup>*Department of Chemistry, University of Azad Jammu and Kashmir, Muzffarabad 13100, Pakistan*

<sup>b</sup>*Department of Biology, College of Sciences, Taif University, P.O. Box 11099, Taif 21944, Saudi Arabia*

<sup>c</sup>*Department of Chemistry, College of Science, Taif University, P.O. Box 11099, Taif 21944, Saudi Arabia*

<sup>d</sup>*Department of Chemistry, Hazara University, Mansehra, Pakistan*

<sup>e</sup>*Department of Software Engineering, University of Azad Jammu and Kashmir, Muzffarabad 13100, Pakistan*

The physicochemical characteristics of Zinc nanoparticles (ZnO NPs) were investigated using various techniques after they were produced using the sol gel process. The crystalline structure, surface morphology, optical property, elemental and chemical composition of the samples have been studied by X-diffraction (XRD), scanning electron microscopy (SEM), diffuse reflectance (DRS), energy dispersive X-ray (EDX) and fourier transform infrared (FTIR) spectroscopies respectively. The synthesis of extremely pure, well crystalline and photo-active ZnO NPs with mixed surface morphology was obtained. Afterward, the photocatalytic activity of ZnO NPs were evaluated against Rhodamine 6G (RH-6G) in aqueous medium.

(Received September 4, 2021; Accepted March 22, 2022)

*Keywords:* Zinc oxide, Characterization, Rhodamine 6G, Diffraction, Photocatalysis

### 1. Introduction

In recent years, the textile industry is causing environmental pollution which adversely affect water as they contain organic compounds like herbicides, growth stimulants, pesticides, detergents, benzene compounds, industrial pigments such as hexachlorobenzene, Rhodamine B, methyl orange, methyl blue etc. and many other bacterial and toxic agents [1]. Various viruses, protozoa and bacteria cause many diseases such as giardia, hepatitis, typhoid, cholera and COVID-19. Regular usage of contaminated water causes prolonged illness and carcinogenesis in man and other animals [2].

Photocatalysis is an expensive and eco-friendly method for the degradation of textile dyes because of its electron affinity [3]. Synthesis of metal nanoparticles by green method is suitable for the production of non-toxic material as it is an eco-friendly method [4]. Zinc oxide that possesses 3.1-3.3 eV band gap has applications in antibacterial activity, drug carriers, cosmetics, biosensors and many others [5]. Due to the production of reactive oxygen, zinc oxide nanoparticles can be used against fungal, spoiling bacterial, pathogenic strains and for the remediation of organic pollutants [6,7]. Various methods are used for the synthesis of ZnO nanoparticles such as mechanochemical synthesis, thermal evaporation, spray pyrolysis, microwave method, organometallic synthesis, mechanical milling, homogeneous precipitation and sol-gel method [8-12].

In this study, we are reporting the sol-gel synthesis of ZnO NPs which were characterized by DRS, FTIR, SEM, EDX and XRD. The photocatalytic efficacy of ZnO NPs were evaluated Rh-6G and a set equation was used to derived the photocatalytic parameters.

---

\* Corresponding author: [cii\\_raj@yahoo.com](mailto:cii_raj@yahoo.com)

<https://doi.org/10.15251/DJNB.2022.172.499>

## 2. Experimental section

### 2.1. Materials

The analytical grade chemicals were purchased from Sigma-Aldrich including  $\text{Zn}(\text{NO}_3)_2$ , NaOH and  $\text{C}_2\text{H}_5\text{OH}$  and used without further purification. All the working solution were prepared in deionized water while the glassware were washed with 15% nitric acid solution followed by deionized water.

### 2.2. Synthesis of ZnO NCs

The calculated amount (0.95 g) of  $\text{Zn}(\text{NO}_3)_2$  was dissolved in 500 mL deionized water in order prepared 10 mM solution and 80 mL of the solution was transferred into a beaker containing 20 mL ethanol whereas NaOH solution was added dropwise to attend pH 10 and stirred (250 rpm) and heated (50 °C) till the formation of gel, which was than kept for overnight cooling and washed with deionized water and the oven dried powder was stored in polyethylene bottle for further experiment.

### 2.3. Characterization

The crystal characteristics were investigated using the Panalytical X-Pert Pro X-ray diffraction model. The scanning electron microscopy (SEM) model JEOL 5910 (Japan) was utilised for morphological examination. The percentage composition and purity were investigated using the energy dispersive X-ray (EDX) model INCA 200 (UK) at 20 keV. The diffuse reflectance spectroscopy model lambda 950 with an integrating sphere in the wavelength range 200-1000 nm and the band gap was calculated via Tauc plot. The Nicolet 6700 (USA) spectrometer was utilised for FTIR analysis in the 4000-400  $\text{cm}^{-1}$  range [13].

### 2.4. Photocatalytic activity

The photocatalytic reaction was performed under irradiation of solar light in the month of June (11 am to 3 pm) and 50 mL of Rh-6G solution and 40 mg of the catalyst were transferred to a reactor for each reaction, and the reactor was covered with aluminum foil to avoid sun contact. To achieve adsorption/desorption equilibrium, the beaker was covered with aluminum foil and agitated for 30 minutes. The reaction was then exposed to sun light for a period of time and absorbance maxima was check after specific interval of time [14–16].

## 3. Results and Discussion

### 3.1. Physicochemical study

Diffraction bands at  $2\theta$  position in the XRD spectrum of ZnO NPs (Fig. 1), with corresponding hkl values of 31.87 (100), 34.14 (002), 36.62 (101), 47.48 (102), 56.79 (110), 63.21 (103), and 67.89 (112) matched with reference card 01-079-0205. The hexagonal shape of ZnO NPs was ascribed to these reflections. The production of well-crystalline nanostructures is confirmed by the crisp and strong diffraction bands, and all of the peaks were assigned to the necessary elements, implying that the synthesized samples are extremely pure. The Debye-Scherrer equation determined the crystallite sizes for ZnO NPs at 30.52 nm, with 0.33 percent imperfection in the ZnO crystal.

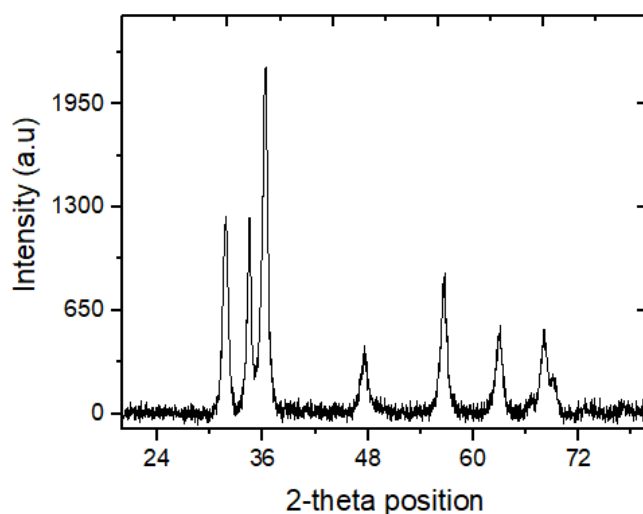


Fig. 1. XRD pattern of ZnO NPs.

The surface structure of ZnO NPs has been examined under SEM and the low and high magnified SEM micrographs are shown in Fig. 2 (a and b). The unevenly distributed mixed shaped particles were seen in the SEM image of ZnO NPs (Fig. 2). It has been observed the large sized particles were formed due to the aggregation of several small particles, which has varied shape and size. Beside larger aggregates, many individual particles with wide-range size and shape are also clearly seen in both images. The individual particles size estimated from the highly magnified SEM image is ranging from 68.47 to 105.82 nm with average particle size of 83.47 nm.

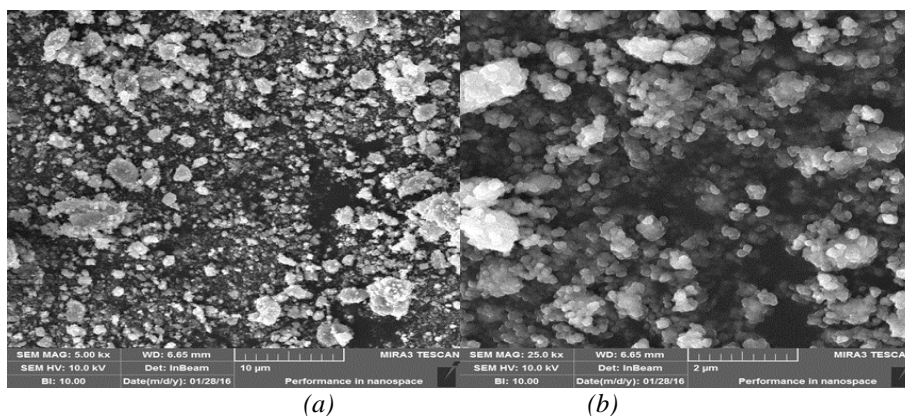


Fig. 2. The low (a) and high (b) magnification SEM micrographs of ZnO NPs.

The existence of three peaks at 0.9, 8.8, and 9.7 keV in the EDX spectrum of ZnO NPs (inset in Fig. 3) indicates the presence of Zn in the sample, but the peak at 0.25 keV assigned to O and the absence of any other peak imply that the ZnO sample is extremely pure. The weight percentage derived by the EDX analysis for Zn and O are 80.3 and 19.7 % respectively. The FTIR spectrum of ZnO NPs shown in Fig.3 possess a wide band centered at  $3436.20\text{ cm}^{-1}$  and  $1647.11\text{ cm}^{-1}$  assigned to O-H stretching. The peak at  $1384.84\text{ cm}^{-1}$  due to the  $\text{NO}_3$ , which is might be due to the used of nitrate salt of Zn in synthesis [17]. The small wide band at  $895.32\text{ cm}^{-1}$  ascribed to O-Zn-O stretching in the lattice whereas the band in the region of  $749\text{-}505\text{ cm}^{-1}$  is responsible for the stretching vibration of Zn-O [18–20].

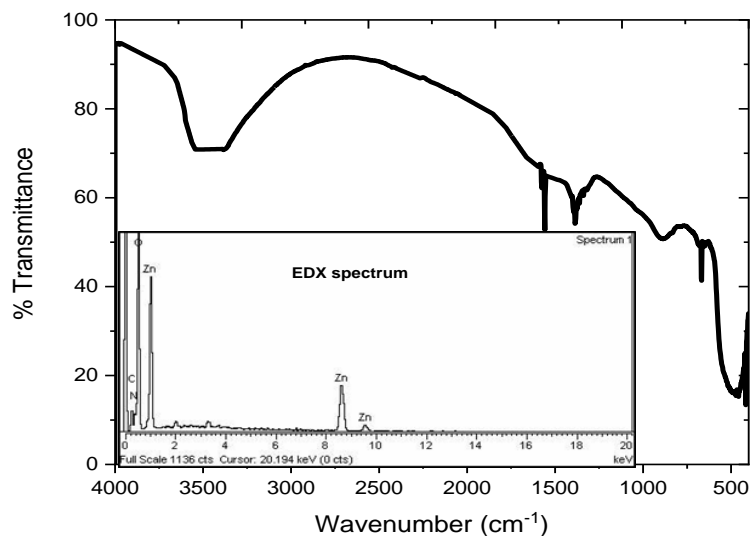


Fig. 3. FTIR spectrum (inset: EDX spectrum) of ZnO NPs.

The transmittance spectra were used to assess the electronic state of the ZnO NPs, revealing that all of the samples are transparent across a wide wavelength range. The optical band gap energies were calculated using the Tauc relation ( $ah\nu=B(h\nu-E_g)^n$ ); where  $h\nu$  is the light intensity,  $a$  is the absorption coefficient,  $B$  is constant, and  $n$  varies depending on the type of transition: direct, forbidden direct, indirect, or forbidden indirect, with values of 1/2, 2, 3/2, or 3 for direct, forbidden direct, indirect, and forbidden indirect, respectively [21]. The DRS spectrum (Fig. 4) of ZnO NPs show decreased transmittance in the UV range (highest absorption). The band gap energy was calculated for ZnO NPs from Tauc plot (inset: Fig. 4) by joining the sharp rising portion with the horizontal axis of the  $(h\nu/nT)^2$  against  $h\nu$  of 3.39 eV [22,23].

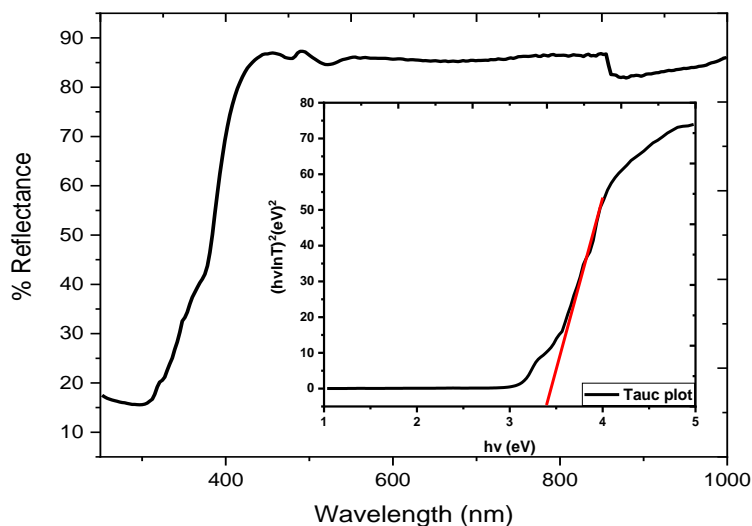


Fig. 4. DRS spectrum (inset: Tauc plot) of ZnO NPs.

### 3.2. Photocatalytic study

In the presence of simulated solar light, the photocatalytic activity of produced ZnO NPs was investigated in the photodegradation of Rh-6G in aqueous solution. The degradation profile shown in Fig.5 (a) demonstrates the degradation of Rh-6G by a progressive reduction in the absorbance maxima at 526 nm. eq. 1 was used to determine the % degradation of, where  $C_0$  and  $C_t$  are the starting and final concentrations of Rh-6G, respectively [24]. In the presence of ZnO NPs,

the percentage degradation of Rh-6G (Fig.5 (b)) is 96.70 percent. The Langmuir-Hinshelwood kinetic model (eq.2) was used to investigate the kinetics of the photocatalytic process, where  $C$  and  $C_0$  are the beginning and final concentrations of Rh-6G, and  $k$  and  $t$  are apparent constants [25]. The straight line produced by plotting  $\ln C/C_0$  vs time in Fig. 5 (c), together with  $r^2$  values of 0.955 for ZnO NPs, indicates that the photocatalytic process follows pseudo 1<sup>st</sup> order kinetics. The photo-degradation rate constants for Rh-6G through ZnO NPs calculated from the slope of linear plot is  $0.938 \times 10^{-2} \text{ min}^{-1}$ .

$$\% \text{ Degradation} = \frac{C_0 - C_t}{C_0} \times 100 \quad (\text{eq.1})$$

$$\ln\left(\frac{C}{C_0}\right) = -kt \quad (\text{eq.2})$$

When an incoming light beam fall on the catalyst surface, an electron excited to the conduction band (CB) from valence band (VB) leaving a positive hole in the VB. The positive hole react with  $\text{OH}/\text{H}_2\text{O}$  molecule producing OH radical, which oxidized the Rh-6G upon reaction. Similarly, the excited electron reacts with  $\text{O}_2$  forming  $\cdot\text{O}^-$ , which intern react with hydrogen led the the formation of OH radical. The dye oxidixed into  $\text{H}_2\text{O}$  and  $\text{CO}_2$ , when reacts with OH radical [24,26].

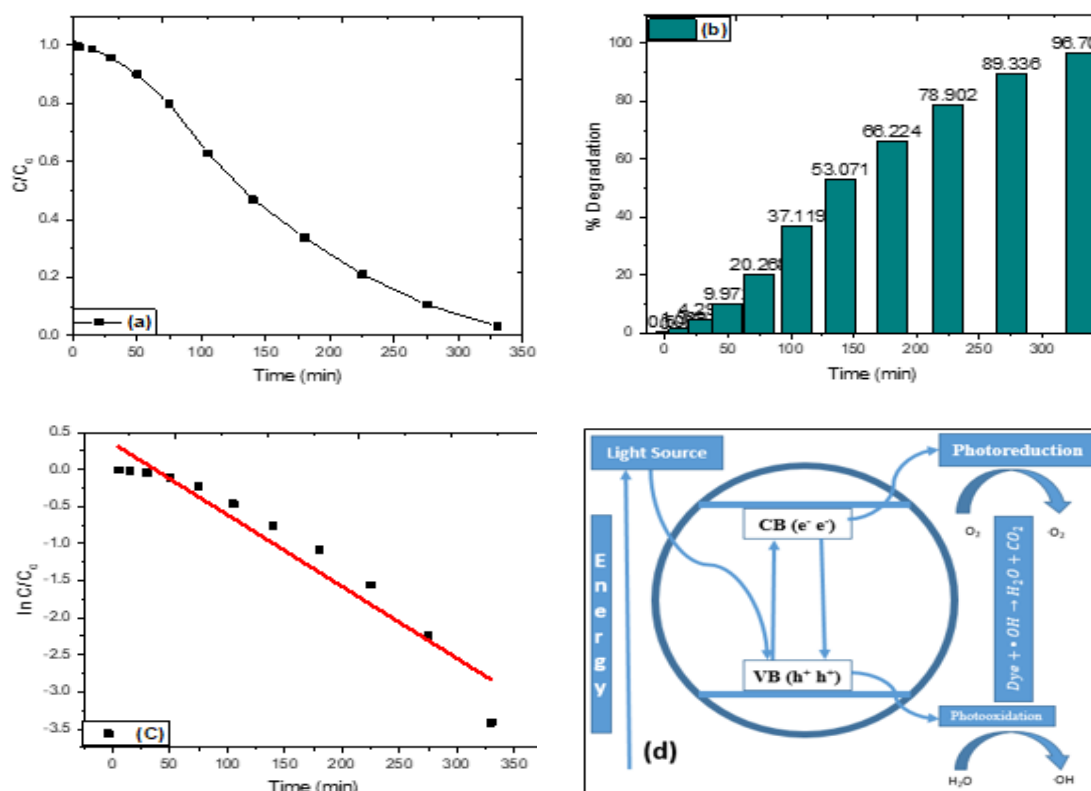


Fig. 5. Degradation profile (a), percent degradation (b),  $\ln C/C_0$  vs  $T$  plot and schematic mechanism electron-hole generation of ZnO NPs.

#### 4. Conclusions

The sol-gel method was utilised to create ZnO NPs, and their physicochemical characteristics were investigated using various approaches. These methods demonstrate the production of well-crystalline nanosized ZnO NPs with a variety of morphological forms. The EDX examination reveals that the required nanostructures are very pure and devoid of impurities.

The band gap energies and other physicochemical characteristics of the produced ZnO NPs influenced their photocatalytic activity. The ZnO NPs was proved is an excellent photo-catalyst for the degradation of organic dye in aqueous medium under the same reaction condition.

## References

- [1] V. V. Pham, T. D. Nguyen, P. Phuong, H. La, *Advances in Natural Sciences: Nanoscience and Nanotechnology* 11, 15005 (2020).
- [2] S. Sarkar, N. Torres, P. Aparna, B. Rajib, B. Saravanan, *Environmental Chemistry Letters* 18, 1569 (2020); <https://doi.org/10.1007/s10311-020-01021-w>
- [3] N. Bibi, S. Haq, W. Rehman, M. Waseem, M. U. Rehman, A. Shah, B. Khan, P. Rasheed, *Biointerface Research in Applied Chemistry* 10, 5895 (2020).
- [4] H. K. Abdelhakim, (2020).
- [5] J. E. Jeronsia, L. A. Joseph, M. M. Jaculine, P. A. Vinosha, S. J. Das, *Journal of Taibah University for Science* 10, 601 (2016); <https://doi.org/10.1016/j.jtusci.2015.12.003>
- [6] I. Matai, A. Sachdev, P. Dubey, S. Uday Kumar, B. Bhushan, P. Gopinath, *Colloids and Surfaces B: Biointerfaces* 115, 359 (2014); <https://doi.org/10.1016/j.colsurfb.2013.12.005>
- [7] M. Anvarinezhad, A. Javadi, 375 (2020); <https://doi.org/10.1515/gps-2020-0040>
- [8] T. Uyen, D. Thi, T. Nguyen, Y. D. Thi, H. Ta, 23899 (2020).
- [9] M. Sorbiun, E. Shayegan, M. Ali, *International Journal of Environmental Research* 12, 29 (2018); <https://doi.org/10.1007/s41742-018-0064-4>
- [10] S. A. Kaur, G. S. Randhawa, R. Singh, 9, 18 (2017).
- [11] S. Akbar, K. S. Haleem, I. Tauseef, W. Rehman, N. Ali, M. Hasan, *Nanoscience and Nanotechnology Letters* 9, 2005 (2017); <https://doi.org/10.1166/nml.2017.2550>
- [12] M. C. Straccia, G. G. D'Ayala, I. Romano, P. Laurienzo, *Carbohydrate Polymers* 125, 103 (2015); <https://doi.org/10.1016/j.carbpol.2015.03.010>
- [13] S. Shoukat, S. Haq, W. Rehman, M. Waseem, M. Hafeez, S. U. Din, Zain-ul-Abdin, P. Ahmad, M. U. Rehman, A. Shah, B. Khan, *Journal of Inorganic and Organometallic Polymers and Materials* (2020).
- [14] S. Haq, W. Rehman, M. Waseem, V. Meynen, S. U. Awan, S. Saeed, N. Iqbal, *Journal of Photochemistry and Photobiology B: Biology* 186, 116 (2018); <https://doi.org/10.1016/j.jphotobiol.2018.07.011>
- [15] S. Shoukat, S. Haq, W. Rehman, M. Waseem, M. I. Shahzad, N. Shahzad, M. Hafeez, S. U. Din, Zain-ul-Abdin, A. Shah, P. Rasheed, *Journal of Inorganic and Organometallic Polymers and Materials* 1 (2020).
- [16] S. Haq, W. Rehman, M. Waseem, V. Meynen, S. U. Awan, A. R. Khan, S. Hussain, Zain-ul-Abdin, S. U. Din, M. Hafeez, N. Iqbal, *Journal of Inorganic and Organometallic Polymers and Materials* 31, 1312 (2021); <https://doi.org/10.1007/s10904-020-01810-4>
- [17] L. A. Joseph, P. A. Vinosha, J. E. Jeronsia, M. M. Jaculine, S. J. Das, *Journal of Taibah University for Science* 10, 601 (2015); <https://doi.org/10.1016/j.jtusci.2015.12.003>
- [18] A. Sharma, S. Kumar, N. Budhiraja, M. Singh, *Advances in Applied Science Research* 4, 252 (2013).
- [19] A. Alhadhrami, A. S. A. Almalki, A. M. A. Adam, M. S. Refat, 13, 6503 (2018).
- [20] E. Zare, S. Pourseyedi, M. Khatami, E. Darezereshki, *Journal of Molecular Structure* 1146, 96 (2017); <https://doi.org/10.1016/j.molstruc.2017.05.118>
- [21] M. Dehbashi, M. Aliahmad, *International Journal of Physical Sciences* 7, 5415 (2012).
- [22] F. Gu, S. F. Wang, C. F. Song, M. K. Lü, Y. X. Qi, G. J. Zhou, D. Xu, D. R. Yuan, *Chemical Physics Letters* 372, 451 (2003); [https://doi.org/10.1016/S0009-2614\(03\)00440-8](https://doi.org/10.1016/S0009-2614(03)00440-8)
- [23] V. Vinoth, T. Sivasankar, A. M. Asiri, J. J. Wu, K. Kaviyaran, S. Anandan, *Ultrasonics*

- Sonochemistry 51, 223 (2018); <https://doi.org/10.1016/j.ultsonch.2018.10.022>
- [24] A. Shah, S. Haq, W. Rehman, W. Muhammad, S. Shoukat, M. ur Rehman, Materials Research Express 6, 045045 (2019); <https://doi.org/10.1088/2053-1591/aafd42>
- [25] S. Shoukat, W. Rehman, S. Haq, M. Waseem, A. Shah, Materials Research Express 6, 115052 (2019); <https://doi.org/10.1088/2053-1591/ab473c>
- [26] P. Rasheed, S. Haq, M. Waseem, S. U. Rehman, W. Rehman, N. Bibi, S. A. A. Shah, Materials Research Express 7, (2020); <https://doi.org/10.1088/2053-1591/ab6fa2>